Available online at www.sciencedirect.com
ScienceDirect
International Journal of Heat and Mass Transfer 50 (2007) 1771–1780
International Journal of HEAT and MASS TRANSFER
www.elsevier.com/locate/ijhmt

Effect of sinusoidal wavy bottom surface on mixed convection heat transfer in a lid-driven cavity

Abdalla Al-Amiri [a], Khalil Khanafer [b], Joseph Bull [b], Ioan Pop [c,*]

[a] Mechanical Engineering Department, United Arab Emirates University, UAE
[b] Biomedical Engineering Department, University of Michigan, Ann Arbor, MI 48109, USA
[c] Faculty of Mathematics, University of Cluj, R-3400 Cluj, Romania

Received 17 April 2006
Available online 30 November 2006

Abstract

The current numerical study is conducted to analyze mixed convection heat transfer in lid-driven cavity with a sinusoidal wavy bottom surface. The cavity vertical walls are insulated while the wavy bottom surface is maintained at a uniform temperature higher than the top lid. In addition, the transport equations are solved using the finite element formulation based on the Galerkin method of weighted residuals. The validity of the numerical code used is ascertained by comparing our results with previously published results. The implications of Richardson number, number of wavy surface undulation and amplitude of the wavy surface on the flow structure and heat transfer characteristics are investigated in detail while the Prandtl number is considered equal to unity. The trend of the local heat transfer is found to follow a wavy pattern. The results of this investigation illustrate that the average Nusselt number increases with an increase in both the amplitude of the wavy surface and Reynolds number. Furthermore, optimum heat transfer is achieved when the wavy surface is designated with two undulations while subjected to low Richardson numbers.

1. Introduction

Mixed convection flow and heat transfer in lid-driven cavities have been receiving a considerable attention in the literature. This attention stems from its importance in vast technological, engineering, and natural applications. Such applications include cooling of electronic devices, lubrication technologies, drying technologies, food processing, float glass production [1], flow and heat transfer in solar ponds [2], thermal–hydraulics of nuclear reactors [3], and dynamics of lakes [4]. Flow and heat transfer phenomena caused by buoyancy and shear forces in enclosures have been studied extensively in the literature. Understanding of these two competing mechanisms is of great significance from both fundamental and practical standpoints. The lid-driven cavity problem has been extensively used as a benchmark case for the evaluation of numerical solution algorithms [5–9]. In fact, the literature shows that two categories of studies were analyzed [10]. The first category is concerned with a horizontal sliding lid which encompasses the top wall [11–16], bottom sliding wall [17] or an oscillating lid [18–20]. The second category is associated with side driven differentially-heated enclosures, where one wall or both vertical walls move with a constant velocity [21–23].

Flow and heat transfer from irregular surfaces are often encountered in many engineering applications to enhance heat transfer such as micro-electronic devices, flat-plate solar collectors and flat-plate condensers in refrigerators [24], and geophysical applications (e.g., flows in the earth's crust [25]), underground cable systems, electric machinery, cooling system of micro-electronic devices, etc. In addition, roughened surfaces could be used in the cooling of electrical and nuclear components where the wall heat flux is known. Surfaces are intentionally roughened sometimes to enhance heat transfer. It is worth noting that most of

* Corresponding author.
E-mail address: pop.ioan@yahoo.co.uk (I. Pop).

0017-9310/$ - see front matter © 2006 Elsevier Ltd. All rights reserved.
doi:10.1016/j.ijheatmasstransfer.2006.10.008

Nomenclature

A	dimensionless amplitude of the wavy surface
g	gravitational acceleration
Gr	Grashof number, $Gr = g\beta(T_H - T_C)H^3/\nu^2$
h	heat transfer coefficient
H	side length of the enclosure
k	thermal conductivity
Nu	Nusselt number
P	dimensionless pressure
Pr	Prandtl number, ν/α
Re	Reynolds number, U_0H/ν
Ri	Richardson number, Gr/Re^2
T	temperature
S	total chord length of the wavy surface
u, v	velocity components along x- and y- axes
U, V	dimensionless velocity components
U_0	sliding top wall velocity
x, y	Cartesian coordinates
X, Y	dimensionless coordinates

Greek symbols

α	thermal diffusivity
β	volumetric expansion coefficient
λ	number of undulation
ν	fluid kinematic viscosity
θ	dimensionless temperature, $(T - T_{cold})/(T_{hot} - T_{cold})$
ρ	fluid density
Ω	dimensionless vorticity, $\omega H/U_0$
Ψ	dimensionless stream function, ψ/HU_0

Subscripts

cold	cold wall
hot	hot wall

the previous studies on enclosures with a form of wavy surfaces were concerned with natural convection. For example, Das and Mahmud [25] conducted a numerical investigation of natural convection in an enclosure consisting of two isothermal horizontal wavy walls and two adiabatic vertical straight walls. Also, Adjlout et al. [26] have studied laminar natural convection in an inclined cavity with a heated undulated wall, i.e., smooth wave-like pattern. Their results concluded that the hot wall undulation affects the flow and heat transfer rate in the enclosure in which the local Nusselt number distribution results in a decrease of heat transfer rate as compared with the square enclosure. Moreover, Kumar [27] conducted a study of flow and thermal field inside a vertical wavy enclosure filled with a porous media. The author has illustrated that the surface temperature was very sensitive to the drifts in the surface undulations, phase of the wavy surface and the number of considered waves.

Our survey of literature has shown few studies have considered the implications of complex geometries on the momentum and energy transport processes under mixed convection heat transfer regime. The corrugated wall channel is one of several devices used for enhancing heat transfer characteristics of many industrial transport processes. It should be pointed out that viscous flow in wavy channels was first analyzed analytically by Bums and Parkes [28] while Goldstein and Sparrow [29] used the naphthalene technique to measure local and average heat transfer coefficients in a corrugated wall channel. Furthermore, O'Brien and Sparrow [30] performed an experimental study to determine forced convection heat transfer coefficients and friction factors for flows in a corrugated duct for Reynolds number, based on the duct hydraulic diameter, ranged from 1,500 to 25,000 with a Prandtl number in the range between 4 and 8. The subsequent enhancement in heat transfer was reported to be approximately two and a half times that reported for a classical parallel-plate channel. In addition, Wang and Chen [31] analyzed forced convection in a wavy-wall channel and demonstrated the effects of wavy geometry, Reynolds number and Prandtl number on the skin friction and Nusselt number. Their results have illustrated that the amplitudes of skin friction coefficient and Nusselt number had increased with an increase in the amplitude to wavelength ratio.

To the best of the authors' knowledge, no attention has been paid to the problem of mixed convection of flow and heat transfer in a lid-driven cavity that is heated from a wavy bottom surface. The objective of the present study is to examine the momentum and energy transport processes in a lid-driven cavity with wavy bottom surface. The cavity is sustained under a vertical temperature gradient by subjecting the bottom wall to a relatively higher temperature than the top lid. The results are shown in terms of parametric presentations of streamlines and isotherms for various considered pertinent dimensionless parameters. These dimensionless groups include the Richardson number, the wavy surface amplitude, and number of undulations offered by the wavy bottom surface. Finally, the implications of the above dimensionless parameters are also depicted on the dimensionless local heat flux and the global Nusselt number predictions.

2. Problem formulation

The treated problem is a two-dimensional square cavity with a side length H. The physical system considered in the present study is displayed in Fig. 1. The vertical walls are considered adiabatic and impermeable while the horizontal

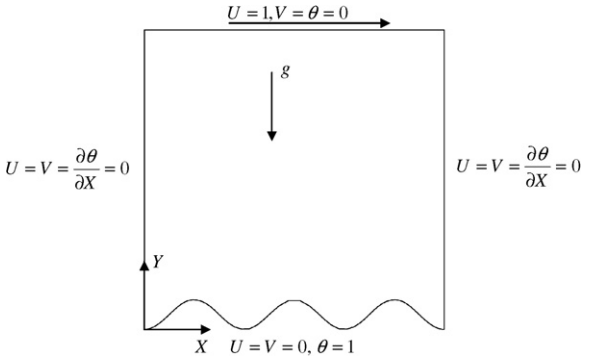

Fig. 1. Schematic diagram of the cavity and boundary conditions.

walls are maintained at uniform but different temperatures such that the bottom wall is assigned to temperature T_{hot} while the top wall is subjected to temperature T_{cold}. Under all circumstances $T_{\text{hot}} > T_{\text{cold}}$ condition is maintained. Furthermore, the top wall is assumed to slide from left to right at a constant speed U_0. In addition, the working fluid is assumed to be Newtonian and incompressible with the flow is set to operate in the laminar mixed convection regime. The fluid properties are assumed constant except for the density variation which is treated according to Boussinesq approximation while viscous dissipation effects are considered negligible. The viscous incompressible flow and the temperature distribution inside the cavity are described by the Navier–Stokes and the energy equations, respectively. The governing equations were transformed into dimensionless forms upon incorporating the following non-dimensional variables:

$$(X, Y) = \frac{(x, y)}{H},\ (U, V) = \frac{(u, v)}{U_0},\ \theta = \frac{T - T_{\text{cold}}}{T_{\text{hot}} - T_{\text{cold}}} \tag{1}$$

where X and Y are the dimensionless coordinates measured along the horizontal and vertical axes, respectively, u and v being the dimensional velocity components along x- and y-axes, and θ is the dimensionless temperature. The dimensionless forms of the governing equations under steady state condition are expressed in the following canonical forms:

$$\nabla . V = 0 \tag{2}$$

$$(V.\nabla)V = \frac{1}{Re}\nabla^2 V + \frac{Gr}{Re^2}(\theta) - \frac{\nabla P}{Re} \tag{3}$$

$$V.\nabla\theta = \frac{1}{PrRe}\nabla^2\theta \tag{4}$$

where V is the velocity vector, P is the dimensionless pressure, Pr is the Prandtl number, $Re = U_0 H/v$ is the Reynolds number, with v being the kinematic viscosity. The strength of the imposed temperature gradient is given by the presentation of the Grashof number Gr defined as

$$Gr = g\beta(T_{\text{hot}} - T_{\text{cold}})H^3/v^2 \tag{5}$$

Here, g is the gravitational acceleration and β is the volumetric coefficient of expansion. It is worth noting that the above governing equations are a combination of mixed elliptic–parabolic system of equations, which need to be solved simultaneously in case of adopting the primitive variable formulation approach. The shape of the bottom wavy surface profile is assumed to mimic the following pattern

$$Y = A[1 - \cos(2\lambda\pi X)] \tag{6}$$

where A is the dimensionless amplitude of the wavy surface and λ is the number of undulation. The definition of the problem at hand is completed by highlighting the applied boundary conditions, which can be summarized as follows:

$$\begin{aligned}
&U = V = 0, \quad \theta = 1 \quad \text{at } Y = 0, 0 < X < 1\\
&U = 1, V = 0, \quad \theta = 0 \quad \text{at } Y = 1, 0 < X < 1\\
&U = V = 0, \quad \frac{\partial\theta}{\partial X} = 0 \quad \text{at } X = 0, 0 \leqslant Y \leqslant 1\\
&U = V = 0, \quad \frac{\partial\theta}{\partial X} = 0 \quad \text{at } X = 1, 0 \leqslant Y \leqslant 1
\end{aligned} \tag{7}$$

In the current investigation, the vorticity-stream function formulations are employed such that

$$U = \frac{\partial\Psi}{\partial Y}, \quad V = -\frac{\partial\Psi}{\partial X}, \quad \Omega = \frac{\partial V}{\partial X} - \frac{\partial U}{\partial Y} \tag{8}$$

$$\Omega = -\nabla^2\Psi \tag{9}$$

where Ω and Ψ are the dimensionless vorticity and stream function, respectively, and are defined as

$$\Omega = \frac{\omega H}{U_0}, \Psi = \frac{\psi}{HU_0} \tag{10}$$

where ω is the dimensional vorticity and ψ is the dimensional stream function. The vorticity-stream function formulation allows the Navier–Stokes equations to be decoupled into one elliptic equation and one parabolic equation which can be solved sequentially. Thus, the dimensionless governing equations can be mathematically expressed as

$$\left(U\frac{\partial\Omega}{\partial X} + V\frac{\partial\Omega}{\partial Y}\right) = \frac{1}{Re}\left(\frac{\partial^2\Omega}{\partial X^2} + \frac{\partial^2\Omega}{\partial Y^2}\right) + Ri\left(\frac{\partial\theta}{\partial X}\right) \tag{11}$$

$$\left(U\frac{\partial\theta}{\partial X} + V\frac{\partial\theta}{\partial Y}\right) = \frac{1}{RePr}\left(\frac{\partial^2\theta}{\partial X^2} + \frac{\partial^2\theta}{\partial Y^2}\right) \tag{12}$$

where $R_i = Gr/Re^2$ is the Richardson number. The range of Richardson numbers considered in the ongoing investigation is $0.01 \leqslant Ri \leqslant 10$, while Prandtl and Grashof numbers are set equal to a fixed value of 0.71 and 10^4, respectively. The vorticity values at the solid boundaries are expressed in terms of the primitive velocity variables such that

$$\begin{aligned}
&\Omega = \frac{\partial V}{\partial X} \quad \text{at } Y = 0, 1;\ 0 < X < 1\\
&\Omega = -\frac{\partial U}{\partial Y} \quad \text{at } X = 0, 1;\ 0 \leqslant Y \leqslant 1
\end{aligned} \tag{13}$$

The rate of heat transfer is computed at the bottom wall and is expressed in terms of the local Nusselt number Nu as

$$Nu = \frac{hH}{k} = -\frac{\partial\theta}{\partial n}H \tag{14}$$

where, h represents the heat transfer coefficient, k thermal conductivity and n the coordinate direction normal to the surface. The dimensionless normal temperature gradient can be written as

$$\frac{\partial\theta}{\partial n} = \frac{1}{H}\sqrt{\left(\frac{\partial\theta}{\partial X}\right)^2 + \left(\frac{\partial\theta}{\partial Y}\right)^2} \tag{15}$$

while the average Nusselt number ($\overline{Nu}$) is obtained by integrating the local Nusselt number along the bottom wavy surface and is defined by

$$\overline{Nu} = \frac{1}{S}\int_0^S Nu\,ds \tag{16}$$

where S is the total chord length of the wavy surface and s is the coordinate along the wavy surface.

3. Numerical scheme

A finite element formulation based on the Galerkin method is employed to solve the governing equations subject to the boundary conditions for the present study. The application of this technique is well documented by Taylor and Hood [32] and Gresho et al. [33]. In the current investigation, the continuum domain is divided into a set of non-overlapping regions called elements. Nine node quadrilateral elements with bi-quadratic interpolation functions are utilized to discretize the physical domain. Moreover, interpolation functions in terms of local normalized element coordinates are implemented to approximate the dependent variables within each element. Subsequently, substitution of the approximations into the system of the governing equations and boundary conditions yields a residual for each of the conservation equations. These residuals are then reduced to zero in a weighted sense over each element volume using Galerkin method.

The highly coupled and non-linear algebraic equations resulting from the discretization of the governing equations are solved using an iterative solution scheme called the segregated-solution algorithm. The advantage of using this method is that the global system matrix is decomposed into smaller submatrices and then solved in a sequential manner. This technique results in considerably fewer storage requirements. A pressure projection algorithm is utilized to obtain a solution for the velocity field at every iteration step. The pressure projection version of the segregated

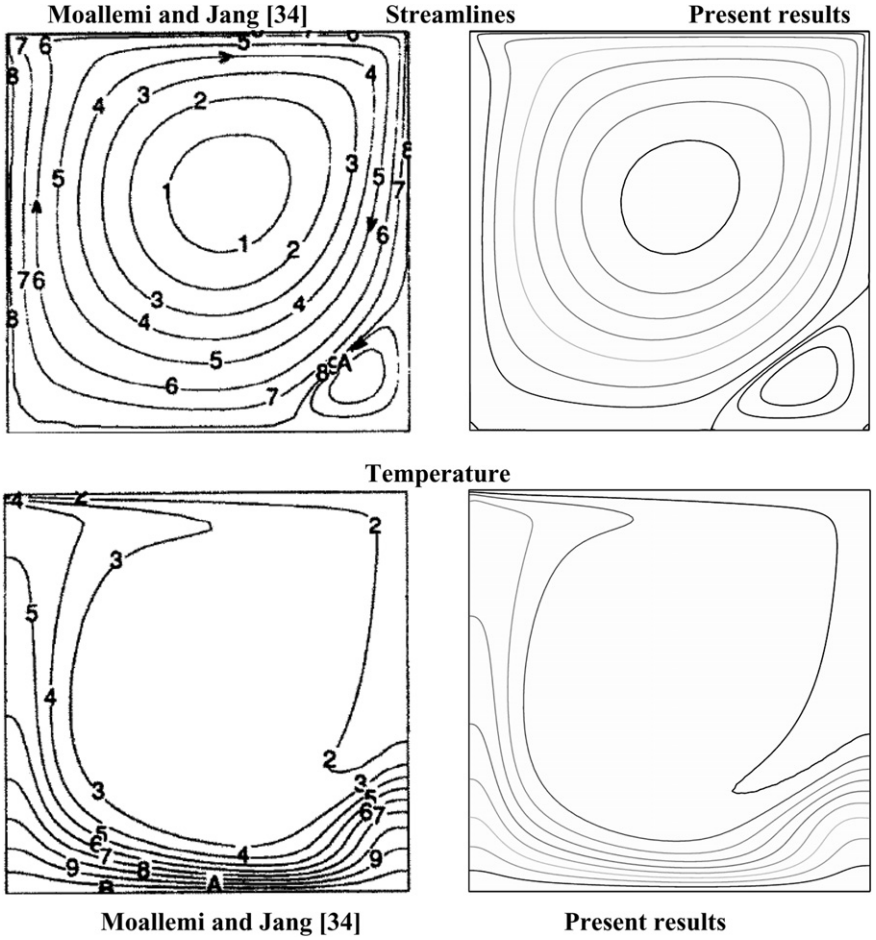

Fig. 2. Comparison of the streamlines and temperature contours between the present work and that of Moallemi and Jang [34] using $Re = 500$, $Ri = 0.4$ and $Pr = 1$.

algorithm is used to solve the non-linear system. In addition, the conjugate residual scheme is used to solve the symmetric pressure-type equation systems, while the conjugate gradient squared method is used for the non-symmetric advection-diffusion-type equations.

A variable grid-size system is generated in the present investigation to capture the rapid changes in the dependent variables. Extensive numerical experimentation is performed to attain grid-independent results. Steady state solution was declared when the relative change in the stream function, vorticity, and temperature fields between two consecutive iterations is satisfied by the following criterion:

$$\sum \left|\varphi_{i,j}^{\gamma+1} - \varphi_{i,j}^{\gamma}\right| \Big/ \sum \left|\varphi_{i,j}^{\gamma+1}\right| \leqslant 10^{-6} \tag{17}$$

where $\varphi_{i,j}^{\gamma}$ stands for stream function, vorticity, and temperature at iteration γ.

4. Model validation

The model validation is an essential part of a numerical investigation. Hence, the outcome of the present numerical code was benchmarked against the numerical results of Moallemi and Jang [34], which were reported for laminar mixed convection heat transfer in a lid-driven cavity heated from below. The comparison was conducted while employing the following dimensionless parameters: $Re = 500$, $Ri = 0.4$ and $Pr = 1$. Excellent agreement was achieved, as illustrated in Fig. 2, between our results and the numerical results of Moallemi and Jang [34] for both the streamlines and temperature contours inside the cavity. Further validation was performed by comparing the local Nusselt number distribution along the cavity lid between the present work and that of Moallemi and Jang [34]. Again, the comparison strikes excellent agreement between both results as displayed in Fig. 3. These validations boost the confidence in our numerical code to carry on with the above stated objectives of the current investigation.

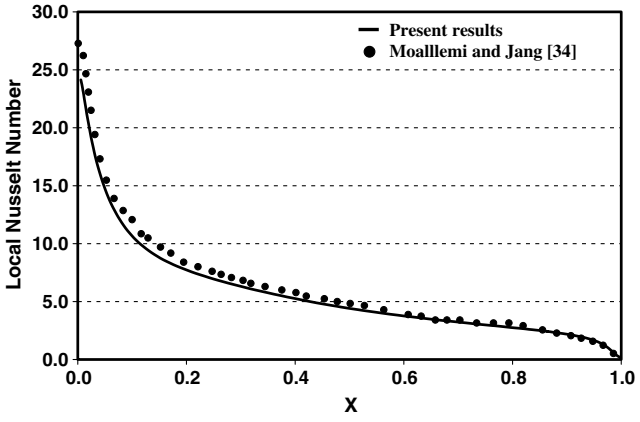

Fig. 3. Comparison of the local Nusselt number variation along the cavity lid between the present results and that of Moallemi and Jang [34] using $Re = 500$, $Ri = 0.4$ and $Pr = 1$.

5. Results and discussion

The characteristics of the flow and temperature fields in the lid-driven cavity are examined by exploring the effects of the Richardson number Ri, number of undulations λ, and amplitude of the wavy bottom surface A. Such field variables are examined by outlaying the steady state version of the streamline and temperature distributions as well as the local heat flux and the average Nusselt number. In the current numerical investigation, the following parametric domains of the dimensionless groups are considered: $0.01 \leqslant Ri \leqslant 10$, $0 \leqslant \lambda \leqslant 3$ and $0 \leqslant A \leqslant 0.075$. In addition, the maximum and minimum recirculation intensity levels and dimensionless temperature bounds were documented for the presented streamline results to reflect on the flow intensity levels.

First, the impact of varying the Richardson number Ri on the streamlines and temperature contours for various numbers of undulations is gauged through the results illustrated in Figs. 4–6 for $A = 0.05$. The Richardson number provides a measure for the importance of the thermal natural convection forces relative to the mechanically induced lid-driven forced convection effect. Again, the considered domain of Ri was varied between 0.01 and 10, which very much spans over a wide range of possible operating conditions. For $Ri = 0.01$, the overall features of the streamlines and temperature contours are similar to those of conventional mechanically-driven cavity flow which are characterized by a primary recirculating clockwise vortex that occupies the bulk of the cavity. In addition, minor vortices tend to form near the bottom corners, which can be captured by increasing the number of contour lines. Meanwhile, thinner boundary layers are depicted to form near the bottom wall. This is attributed to the increase in the contribution of convection heat transfer mechanism, which causes steep temperature gradients in the vertical direction near the bottom wall as shown in Fig. 4. In the bulk of the cavity, however, the temperature differences are very small and consequently the temperature gradients are weak due to the significant effect of the mechanically-induced sliding lid. When the Richardson number increases to unity, the buoyancy effect balances the effect of the sliding top wall and, hence, the total heat transfer in the cavity is controlled by the combined mechanisms of forced and natural convection as shown in Fig. 5. Apparently, the flow activities have weakened as interpreted from the registered minimum and maximum intensity levels. Consequently, the conduction contribution to the overall heat transfer enlarges as illustrated by the expansion of the thermal boundary layers formation above the bottom wall. Upon further increasing the Ri value to 10, the buoyancy effect outweighs the effect of the sliding wall as shown in Fig. 6. Less energy is noticed to be carried away from the sliding top wall into the cavity and, subsequently, the conduction heat transfer regime has become the dominant mode of energy transport in the cavity.

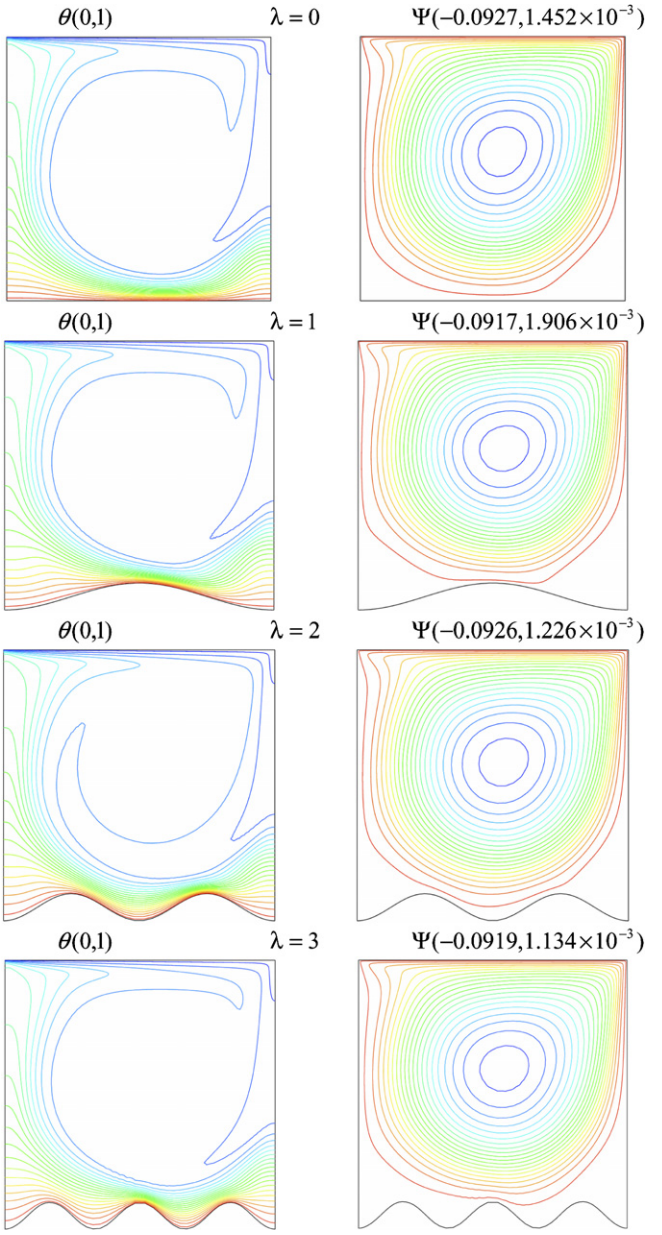

Fig. 4. Streamline and temperature contours for various undulations ($Gr = 10^4$, $Ri = 0.01$).

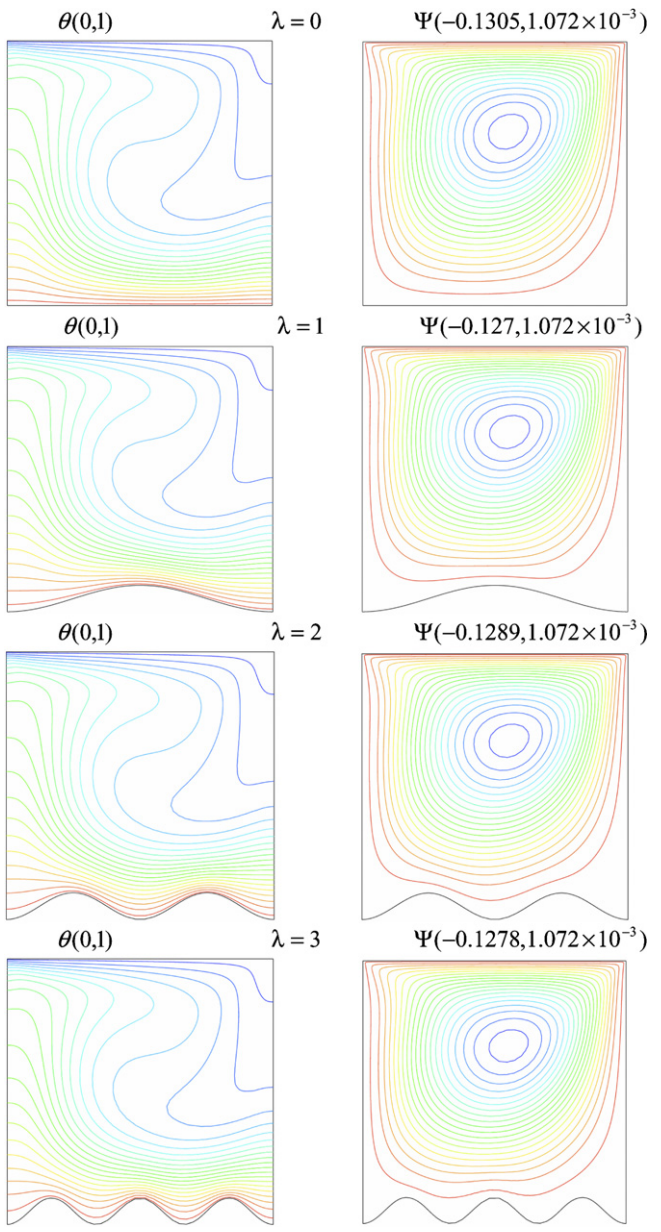

Fig. 5. Streamline and temperature contours for various undulations ($Gr = 10^4$, $Ri = 1$).

Next, the influence of the number of undulations on the local variation of heat along the heated wavy surface is also demonstrated in Figs. 6–8. It appears from the figures that varying the number of undulations λ between 0 and 3 does not disturb the global flow and isotherm patterns except in the vicinity of the bottom wall, where the contour lines mimic the wall's profile. In addition, the recorded upper and lower bounds for flow intensities do not seem to vary significantly either.

Further insight into the effect of the Richardson number and the number of undulations is presented by highlighting their respective effects on the dimensionless local heat flux predictions as shown Figs. 7–9 for $A = 0.05$. It appears that the employed number of undulation impacts the distribution of the local heat flux along arc length of the bottom surface by producing a corresponding number of peaks and valleys which correspond to the imposed n values. It is worth pointing out that the highest local heat flux is achieved with $Ri = 0.01$ which is likely attributed to the heat transfer augmentation offered by the mechanically-sliding lid. Highly localized heat transfer or 'hot spots' might be an issue of concern when low employing low Ri values. Meanwhile, varying Ri value is found to alter the highest attained peak by a given undulation number. The effect of the numbers of undulations n on the average Nusselt number for various Richardson numbers Ri is graphically established Fig. 10. The results show that the average Nusselt number increases with the decrease in the considered Ri value. Moreover, the average Nusselt number is almost uniform for higher Ri values in the considered n

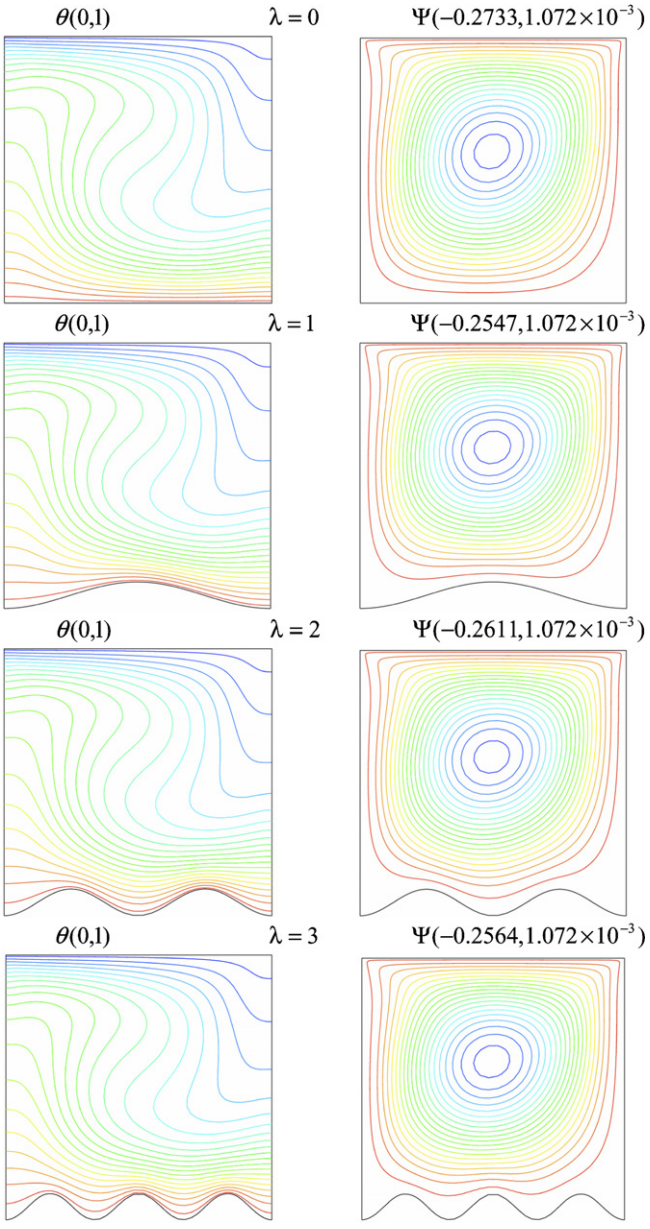

Fig. 6. Streamline and temperature contours for various undulations ($Gr = 10^4$, $Ri = 10$).

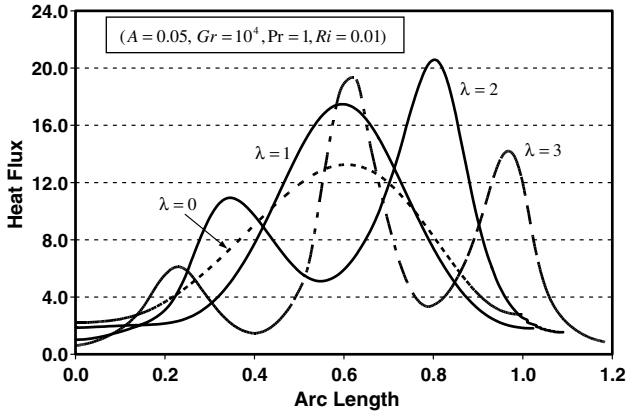

Fig. 7. Local heat flux variation for various numbers of undulations.

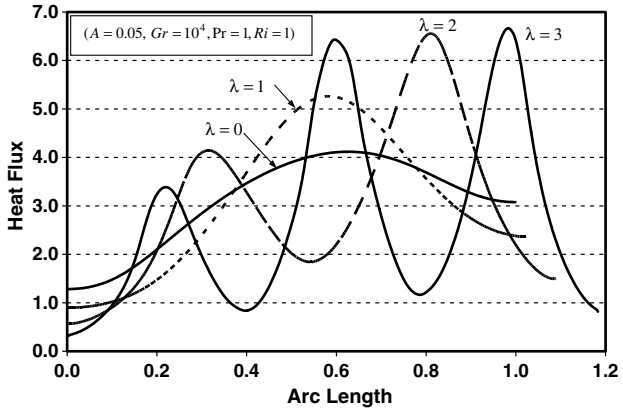

Fig. 8. Local heat flux variation for various numbers of undulations.

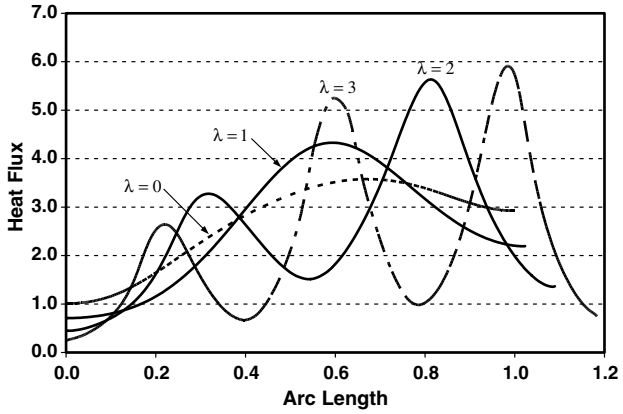

Fig. 9. Local heat flux variation for various numbers of undulations ($A = 0.05$, $Gr = 10^4$, $Pr = 1$, $Ri = 10$).

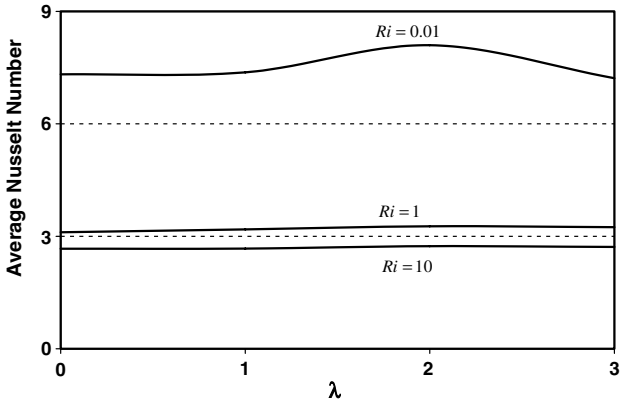

Fig. 10. Effects of Richardson number and the numbers of undulations on the average Nusselt number ($A = 0.05$, $Gr = 10^4$, $Pr = 1$).

range. Such an increase is noticed to be remarkable when incorporating $Ri = 0.01$ owing to the increase in the convection heat transfer contribution to the overall energy transport process. An interesting phenomenon is observed at $Ri = 0.01$ for which the average Nusselt number peaks at $\lambda = 2$ which reflects the high local heat flux distribution as reported in Fig. 7.

The current investigation is wrapped by evaluating the implications of the wavy surface amplitude A on the momentum and energy transport processes in the lid-driven cavity. This is first examined by plotting the streamlines and temperature contours as illustrated in Fig. 11. The results, which are depicted for $Ri = 1$ and $\lambda = 3$, indicate that the flow activities and thermal currents are both a weak function of surface amplitude in the considered rage of $A = 0$–0.075 This effect is more profound in Fig. 12 which shows the effect of the amplitude on the local variation of heat flux along the wavy surface. The results in Fig. 12 exhibits higher local heat flux variation with an increase in the amplitude of the wavy surface owing to higher velocity gradients near the top lid which subsequently increases the heat transfer rate. Finally, the effect of varying the amplitude of the wavy surface on the average Nusselt number predicted at the bottom surface is shown in Fig. 13 for various values of Richardson numbers. The results, as shown in the figure, illustrate that the average Nusselt number is in general higher than that predicted for a flat surface. Moreover, the average Nusselt number is found to increase with the elevation in the magnitude of the amplitude value of the wavy surface. The average Nusselt number obtained from the respective incorporated amplitude values manifest high predications at the lower end of the Ri range considered. However, the average Nusselt number predictions approach an asymptotic value with the increase in Ri value. This is most likely attributed to the overwhelming effect of the natural convection regime which suppresses the effect of the surface waviness and the mechanical effect of the top sliding surface.

The average Nusselt number calculated along the sinusoidal bottom surface is correlated in terms of various pertinent parameters including Richardson number ($0.01 \leqslant Ri \leqslant 10$), dimensionless amplitude of the wavy surface ($0 \leqslant A \leqslant 0.075$), and the number of undulation ($0 \leqslant n \leqslant 3$). This correlation can be written as follow

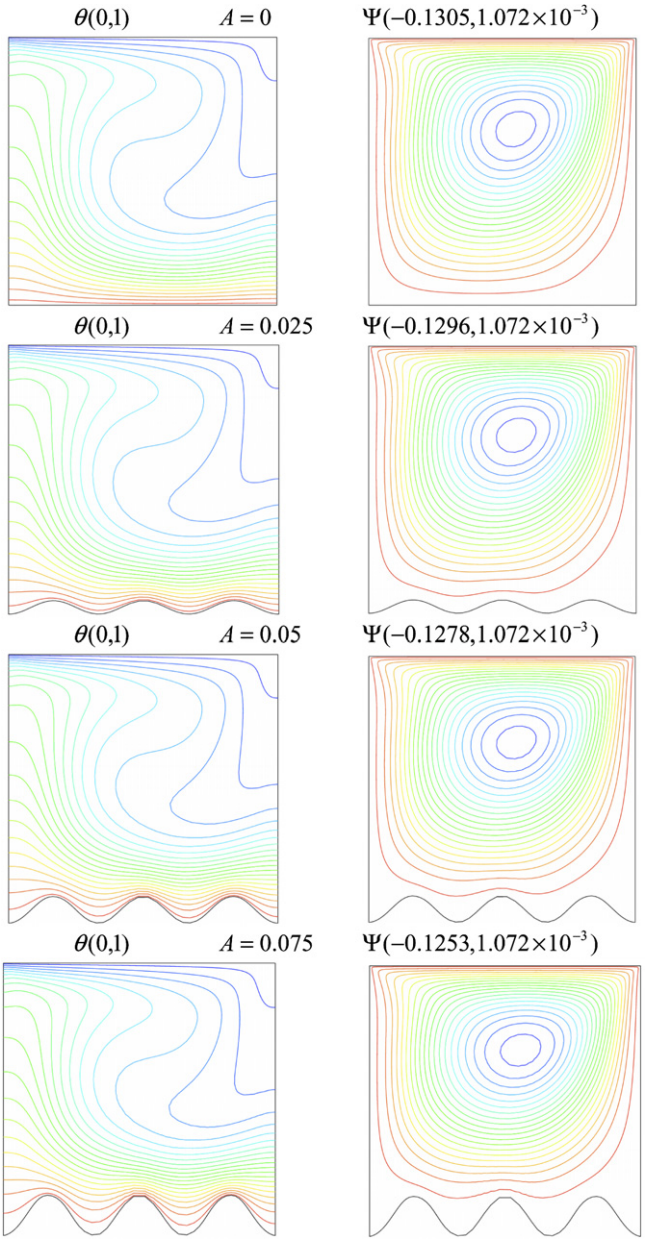

Fig. 11. Streamline and temperature contours for various amplitudes ($Gr = 10^4$, $Ri = 1$).

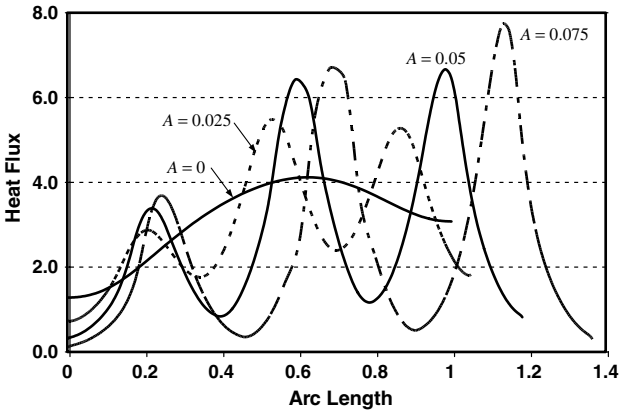

Fig. 12. Local heat flux variation for various amplitudes ($\lambda = 3$, $Gr = 10^4$, $Pr = 1$, $Ri = 1$).

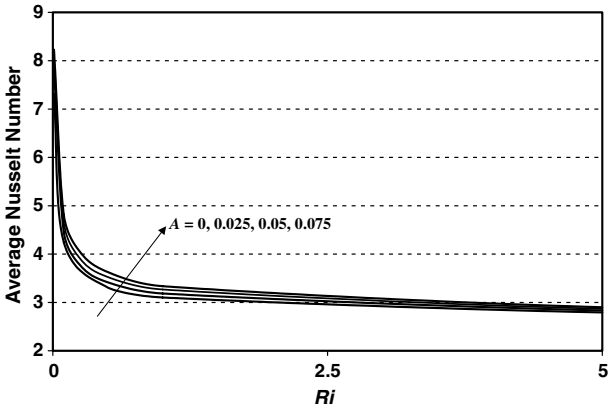

Fig. 13. Effect of the amplitude of the wavy surface on the average Nusselt umber under various Richardson numbers using $Gr = 10^4$ and $\lambda = 2$.

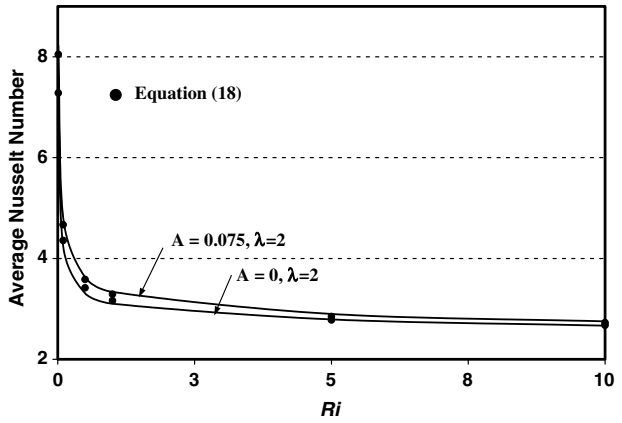

Fig. 14. Comparison of the average Nusselt number between the present numerical results and Eq. (17) for various pertinent parameters.

$$\overline{Nu} = 2.3383 + (6.99 + \lambda)^{0.2417}(A + 0.4848)Ri^{-0.3890} \qquad (18)$$

where the confidence coefficient for the above equation is $R^2 = 99.3\%$. A graphical representation of the above correlation is illustrated in Fig. 14. This figure demonstrates an excellent agreement between the numerical results and those obtained by the correlation.

6. Conclusions

Mixed convection heat transfer in a lid-driven cavity heated from below is studied numerically for various pertinent dimensionless groups. The bottom surface is considered to follow a wavy pattern. Furthermore, the vertical walls were subjected to insulated boundary conditions. The governing equations are solved using the Galerkin finite element method. Effects of dimensionless groups representing the wavy geometry, Richardson number, and number of undulation were highlighted to study their impacts on flow structure and heat transfer characteristics. The increase in the Richardson number hinders flow and thermal current activities owing to the increase in the imposed vertical temperature gradient. Moreover, the results of this investigation have illustrated that the number of undulation at the heated bottom wall significantly affects heat transfer characteristics inside the cavity. The results have also demonstrated that the average Nusselt number was found optimum when employing two undulations at low Richardson number, which can be attained by increasing the sliding lid speed. Finally, the local and average Nusselt number predictions are found to increase with elevation in the amplitude of the wavy surface while maintaining a relatively low Richardson number. Thus, the corrugated lid-driven cavity can be considered as an effective heat transfer mechanism at larger wavy surface amplitudes and low Richardson numbers.

References

[1] L.A.B. Pilkington, Review lecture: The Float Glass Process, third ed., in: Proc. R. Soc. Lond. A, vol. 314, 1969, pp. 1–25.
[2] C.K. Cha, Y. Jaluria, Recirculating mixed convection flow for energy extraction, Int. J. Heat Mass Transfer 27 (1984) 1801–1810.
[3] F.J.K. Ideriah, Prediction of turbulent cavity flow driven by buoyancy and shear, J. Mech. Eng. Sci. 22 (1980) 287–295.
[4] J. Imberger, P.F. Hamblin, Dynamics of lakes, reservoirs, and cooling ponds, Adv. Rev. Fluid Mech. 14 (1982) 153–187.
[5] R.K. Agarwal, A third-order-accurate upwind scheme for Navier–Stokes solutions at high Reynolds numbers, AIAA-81-0112, in: Proc. 19th AIAA Aerospace Sciences Meeting, St. Louis, MO, 1981.
[6] D.L. Young, J.A. Liggett, R.H. Gallagher, Unsteady stratified circulation in a cavity, Eng. Mech. Div. 102 (1976) 1009–1023.
[7] M.C. Thompson, J.H. Ferziger, An adaptive multigrid technique for the incompressible Navier–Stokes equations, Comput. Phys. 82 (1989) 94–121.
[8] U. Ghia, K.N. Ghia, C.T. Shin, High-resolutions for incompressible flow using Navier–Stokes equations and a multigrid method, Comput. Phys. 48 (1982) 387–411.
[9] R. Schreiber, H.B. Keller, Driven cavity flows by efficient numerical techniques, Comput. Phys. 49 (1983) 310–333.
[10] H.F. Oztop, I. Dagtekin, Mixed convection in two-sided lid-driven differentially heated square cavity, Int. J. Heat Mass Transfer 47 (2004) 1761–11769.
[11] R. Iwatsu, J.M. Hyun, Three-dimensional driven-cavity flows with a vertical temperature gradient, Int. J. Heat Mass Transfer 38 (1995) 3319–3328.
[12] A.A. Mohamad, R. Viskanta, Transient low Prandtl number fluid convection in a lid-driven cavity, Num. Heat Transfer: Part A 19 (1991) 187–205.
[13] A.K. Prasad, J.R. Koseff, Combined forced and natural convection heat transfer in a deep lid-driven cavity flow, Int. J. Heat Fluid Flow 17 (1996) 460–467.
[14] C.F. Freitas, R.L. Street, Non-linear transient phenomena in a complex recirculating flow: A numerical investigation, Int. J. Num. Methods Fluids 8 (1988) 769–802.
[15] A.A. Mohamad, R. Viskanta, Flow and heat transfer in a lid-driven cavity with stably stratified fluid, Appl. Math. Model 19 (1995) 465–472.
[16] K.M. Khanafer, A.J. Chamkha, Mixed convection flow in a lid-driven enclosure with a fluid-saturated porous medium, Int. J. Heat Mass Transfer 42 (1999) 2465–2481.
[17] C.-J. Chen, H. Nassari-Neshat, K.-S. Ho, Finite-analytical numerical solution of heat transfer in two-dimensional cavity flow, Num. Heat Transfer 4 (1981) 179–197.
[18] R. Iwatsu, J.M. Hyun, K. Kuwahara, Convection in a differentially-heated square cavity with a torsionally-oscillating lid, Int. J. Heat Mass Transfer 35 (1992) 1069–1076.
[19] R. Iwatsu, J.M. Hyun, K. Kuwahara, Numerical simulation of flows driven by a torsionally oscillating lid in a square cavity, J. Fluids Eng. 114 (1992) 143–149.
[20] Abdalla Al-Amiri, K. Khanafer, I. Pop, Numerical simulation of unsteady mixed convection in a driven cavity using an externally excited sliding lid, Eur. J. Mech. B/Fluids, in press.
[21] V.S. Arpaci, P.S. Larsen, Convection Heat Transfer, Prentice-Hall, 1984, p. 90.
[22] O. Aydın, Aiding and opposing mechanisms of mixed convection in a shear-and buoyancy-driven cavity, Int. Comm. Heat Mass Transfer 26 (1999) 1019–1028.
[23] A.J. Chamkha, Hydromagnetic combined convection flow in a vertical lid-driven cavity with internal heat generation or absorption, Num. Heat Transfer: Part A 41 (2002) 529–546.
[24] J.-H. Jang, W.-M. Yan, Mixed convection heat and mass transfer along a vertical wavy surface, Int. J. Heat Mass Transfer 47 (2004) 419–428.
[25] P.K. Das, S. Mahmud, Numerical investigation of natural convection inside a wavy enclosure, Int. J. Therm. Sci. 42 (2003) 397–406.
[26] L. Adjlout, O. Imine, A. Azzi, M. Belkadi, Laminar natural convection in an inclined cavity with a wavy-wall, Int. J. Heat Mass Transfer 45 (2002) 2141–2152.

[27] B.V.R. Kumar, A study of free convection induced by a vertical wavy surface with heat flux in a porous enclosure, Num. Heat Transfer: Part A 37 (2000) 493–510.
[28] J.C. Bums, T. Parkes, Peristaltic motion, J. Fluid Mech. 29 (1967) 731–743.
[29] J.L. Goldstein, E.M. Sparrow, Heat/mass transfer characteristics for flow in a corrugated wall channel, ASME J. Heat Transfer 99 (1977) 187–195.
[30] J.E. O'Brien, E.M. Sparrow, Corrugated-duct heat transfer, pressure drop, and flow visualization, J. Heat Transfer 104 (1982) 410–416.
[31] C.-C. Wang, C.-K. Chen, Forced convection in a wavy-wall channel, Int. J. Heat Mass Transfer 45 (2002) 2587–2595.
[32] C. Taylor, P. Hood, A numerical solution of the Navier–Stokes equations using finite- element technique, Comput. Fluids 1 (1973) 73–89.
[33] P.M. Gresho, R.L. Lee, R.L. Sani, On the time-dependent solution of the incompressible Navier–Stokes equations in two and three dimensions, in: Recent Advances in Numerical Methods in Fluids, Pineridge, Swansea, UK, 1980.
[34] M.K. Moallemi, K.S. Jang, Prandtl number effects on laminar mixed convection heat transfer in a lid-driven cavity, Int. J. Heat Mass Transfer 35 (1992) 1881–1892.